Available online at www.sciencedirect.com
SCIENCE DIRECT
Journal of Catalysis 233 (2005) 60–67
JOURNAL OF CATALYSIS
www.elsevier.com/locate/jcat

Synthesis and characterization of TM-MCM-48 (TM = Mn, V, Cr) and their catalytic activity in the oxidation of styrene

S. Gómez [a], L.J. Garces [a], J. Villegas [a], R. Ghosh [b], O. Giraldo [d], Steven L. Suib [a,b,c,*]

[a] *Institute of Materials Science, University of Connecticut, Storrs, CN 06269-3060, USA*
[b] *Department of Chemistry, University of Connecticut, Storrs, CN 06269-3060, USA*
[c] *Department of Chemical Engineering, University of Connecticut, Storrs, CN 06269-3060, USA*
[d] *Departamento de Física y Química, Universidad Nacional de Colombia, Manizales, Colombia*

Received 28 January 2005; revised 6 April 2005; accepted 11 April 2005

Available online 23 May 2005

Abstract

Transition-metal (TM) species (Mn, V, and Cr) were incorporated by an anion-exchange method into MCM-48. The TM-MCM-48 materials were characterized by XRD, HRTEM, N_2 adsorption–desorption, ESR, Raman, and NH_3-TPD. The structural and textural properties of the materials are discussed, as is the nature of the TM species introduced in the mesoporous host. The catalytic activity and selectivity of the TM-MCM-48 in the oxidation of styrene with TBHP as an oxidant agent are explored. All of the catalysts produce benzaldehyde and styrene oxide as the main products. Mn-MCM-48 showed the highest selectivity for styrene oxide, but with a maximum conversion of 58%. V-MCM-48 shows the highest conversion of styrene (100%) and the highest selectivity (88%) for benzaldehyde. The Cr catalyst shows the poorest performance in terms of selectivity. The TM-MCM-48 catalysts are very active in the oxidation of styrene, and their activity depends on the nature of the transition metal used.

Keywords: Transition metal; Modified MCM-48; Styrene oxidation

1. Introduction

One of the fastest-developing areas in molecular sieve science is the synthesis of transition-metal-containing molecular sieves. Since the discovery of periodic mesoporous silica M41S materials in 1992 [1], a wide variety of new materials have been synthesized to exploit the ability of these substrates to act as hosts of inorganic and organic species. The most widely researched members of the M41S family are MCM-41 and MCM-48. MCM-41 consists of a hexagonal array and has a unidirectional pore structure, and MCM-48 consists of a cubic array with a three-dimensional pore network [2]. Whereas mesoporous M41S silicate materials do not exhibit flexible oxidation state behavior, the capacity of transition metals to have variable oxidation states expands the potential of M41S materials to be used in catalytic applications. The encapsulation of transition-metal species can also lead to physical properties different from those observed for the bulk guest species. Thus, many studies have concentrated on the introduction of catalytically active sites such as metals and metal complexes into mesoporous silica materials.

Many different synthetic procedures have been developed to incorporate transition metals such as Ti [3–5], Mn [6–11], Cr [5,6,12–15], V [5,6,15,16], into M41S mesoporous silica materials. One of the most popular methods of incorporating metals into mesoporous silica is the direct hydrothermal (DHT) method, which consists of the direct addition of metal ion precursors to the synthesis gel before the hydrothermal synthesis takes place [16]. Other methods, like conventional wet impregnation and grafting, have also been used. More recently Yonemitsu and co-workers developed the template ion-exchange (TIE) method, in which the metal is incorpo-

* Corresponding author.
E-mail address: suib@uconnvm.uconn.edu (S.L. Suib).

0021-9517/$ – see front matter
doi:10.1016/j.jcat.2005.04.015

rated by exchange of the template cations in the channels of as-synthesized MCM-41 with the metal ions in solution [8]. Recently our group developed a new synthetic method for incorporating manganese species in MCM-48 materials [17], which consists of ion-exchanging the negatively charged ions contained in the channels of as-synthesized MCM-48 with high-valence metal precursor anions contained in solution. This method allowed a controlled and high loading of Mn species with variable oxidation state. Since the incorporation of the transition metals takes place in surfactant containing MCM-48, the majority of the Mn incorporated locates inside the pores, rather than in the framework. Most works report incorporation of metals into MCM-41 and fewer into MCM-48. MCM-48, because of its cubic structure, has been suggested to be a more advantageous system than MCM-41 for catalytic applications, since the three-dimensional pore system of MCM-48 could allow faster diffusion through the channels and make this material more resistant to pore blocking [18]. The most useful property of molecular sieves with incorporated transition metals is their redox ability, which can be used in new catalysts for the selective oxidation of a wide range of hydrocarbons.

In this work, we have expanded our previous work to the incorporation of transition metals other than Mn (Cr, V) within the pores of MCM-48. We have studied the nature of the transition-metal species and tested their activity toward oxidation of styrene. Styrene oxidation is of considerable commercial and academic interest for the synthesis of important products such as styrene oxide and phenylacetaldehyde. The influence of the transition metals incorporated and their structural features on catalytic activity and product selectivity in styrene oxidation are investigated.

2. Experimental

2.1. Catalyst synthesis

MCM-48 mesoporous silica was synthesized by a variation of the procedure described by Fröba and co-workers [19]. The synthesis mixture had the following molar ratios: 1 tetraethyl orthosilicate (TEOS):0.65 cetyltrimethylammonium bromide (CTAB):0.5 potassium hydroxide (KOH):62 H_2O. The mixture was stirred for about 20 min and was loaded into a Teflon-lined steel autoclave, where the synthesis solution was statically heated for 4 days at 115 °C. The resultant white products were filtered, washed with deionized water, and dried at room temperature.

The synthesis of the metal-containing materials was performed with an ion-exchange process reported elsewhere [17]. In a typical loading procedure, approximately 200 mg of as-synthesized MCM-48 (surfactant containing) was slurried in water. Then 60 ml of potassium permanganate ($KMnO_4$) (0.05 M) was added to the slurry, and the mixture was stirred for 4 h. Subsequently the Mn-containing MCM-48 was filtered, washed with deionized water, and dried at room temperature. The resulting product was then calcined for 6 h at 500 °C. Potassium permanganate ($KMnO_4$), sodium orthovanadate (Na_3VO_4), and potassium chromate (K_2CrO_4) were used as metal precursors. The materials are referred to here as Mn-MCM-48, V-MCM-48, and Cr-MCM-48.

2.2. Catalyst characterization

Powder X-ray diffraction (XRD) patterns were recorded with a Scintag XDS-2000 diffractometer and Cu-K_α radiation with a voltage of 45 kV and a current of 40 mA.

N_2 sorption experiments were performed to evaluate the textural properties of the catalysts. The experiments were done with a Micrometrics ASAP 2010 analyzer. The samples were degassed at 150 °C overnight before data collection. The surface areas were calculated with the Brunauer–Emmett–Teller (BET) equation, and the pore size distribution was calculated with the use of the desorption branch of the N_2 adsorption-desorption isotherm and the Barret–Joyner–Halenda (BJH) formula.

High-resolution transmission electron microscopy (HRTEM) was performed with a JEOL FasTEM 2010 electron microscope operating at 200 kV, equipped with an EDAX Phoenix EDS analyzer. The samples for analysis were prepared by dispersion of the powdered material in 2-propanol. A drop of the dispersion was then placed on a carbon-coated copper grid and dried.

Electron paramagnetic resonance (EPR) spectra were collected with an X-band (9 GHz) EPR at 298 K on a Bruker EMX spectrometer. The samples were loaded into quartz tubes (3 mm outer diameter, 2 mm interior diameter).

Raman spectra were taken at room temperature in the spectral range of 100–2000 cm^{-1} with a Renishaw 2000 Raman microscope system, which includes an optical microscope and a CCD camera for multichannel detection. The spectra were recorded with the use of a 514-nm argon ion laser.

Ammonia temperature-programmed desorption (NH_3-TPD) was used to evaluate the acidity of the catalysts. In a typical experiment, 30 mg of sample was oven-dried overnight at 110 °C. Then the catalysts were loaded into a quartz tube and pretreated with flowing He (40 ml min^{-1}) at 300 °C for 2 h. After pretreatment the sample was saturated at 80 °C with a 0.5% NH_3/He gas mixture at a flow rate of 40 ml min^{-1} and subsequently flushed with He at 105 °C for 2 h to remove the physisorbed ammonia. NH_3-TPD analysis was carried out from 25 to 750 °C at a heating rate of 10 °C min^{-1}. The desorbed NH_3 was monitored with a MKS-UTI PPT quadrupole mass spectrometer.

2.3. Catalytic activity

The catalytic oxidation of styrene with *tert*-butyl hydroperoxide (TBHP) as an oxidant was carried out in a round-bottomed flask with a magnetic stirrer and a reflux

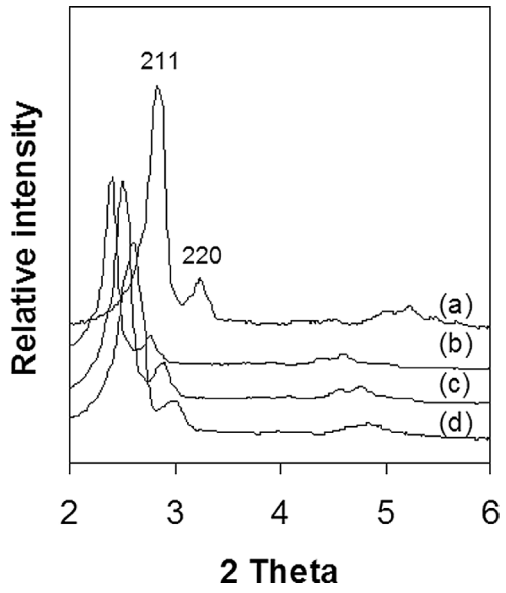

Fig. 1. Powder XRD patterns of calcined (a) MCM-48, (b) Mn-MCM-48, (c) V-MCM-48, and (d) Cr-MCM-48.

condenser. The batch reactor was immersed in a paraffin oil bath to control the temperature. In a typical oxidation reaction, 50 mg of the catalyst was stirred with 2.6 mmol of styrene, 2.6 mmol of TBHP (70 wt% in water) as an oxidizing agent, and 10 ml of acetonitrile as a solvent. The reaction temperature and time were varied from 293 to 353 K and from 6 to 24 h, respectively. The reaction products were analyzed and identified by known standards, with a combined gas chromatography–mass spectrometry (GC-MS) unit with an HP-5MS column (25 m × 0.20 mm × 0.33 μm). Cyclohexyl benzene was used as the internal standard. Leaching of the active components was tested by evaluation of the Si/TM ratio as determined by EDS before and after the oxidation reaction.

3. Results

3.1. Structural and textural characterization

The XRD patterns obtained for the calcined MCM-48 and transition-metal (TM)-containing MCM-48 samples are depicted in Fig. 1. All of the samples show the characteristic low-angle *hkl* reflections of the ordered cubic structure of MCM-48 [20], implying that the cubic mesoporous structure of the parent material is maintained after the TM incorporation. However, a shift to lower 2θ values is observed with TM loading. This behavior was observed before for Mn-MCM-48 samples prepared by the ion-exchange method, where after incorporation of the Mn the shrinkage effect of the silica walls upon calcination is smaller, and thus higher d_{211} values are observed [17]. HRTEM images demonstrate that the cubic arrangement typical of MCM-48 is maintained for all of the catalysts prepared, as shown in Fig. 2. HRTEM analysis also revealed that no other extra phases of the metals are present outside of the mesoporous structure.

Table 1
N_2 sorption results for TM-MCM-48 materials

Catalyst	Si/TM[a]	BET S.A.[b] (m^2/g)	Average P.D.[c] (Å)
MCM-48	n.a.[d]	1056	29
Mn-MCM-48	7	930	34
V-MCM-48	13	1007	37
Cr-MCM-48	19	828	37

[a] Atomic ratios calculated by EDS.
[b] BET surface area.
[c] BJH average pore diameter.
[d] n.a., no applicable.

Fig. 3 and Table 1 show the N_2 sorption results obtained for MCM-48 and TM-MCM-48. The isotherms show the typical trend for mesoporous materials, type IV isotherms in the IUPAC classifications, with a sharp inflection at relative pressure 0.2 to 0.3, which is due to capillary condensation of nitrogen within the pores [21]. All of the materials prepared show reversible adsorption–desorption isotherms. The surface area and pore volume of the catalysts are reduced by the presence of the TM in the mesoporous structure if compared with that of MCM-48 (Table 1); however, for V-MCM-48 the change in surface area compared with the parent material is very small (∼ 5%). The pore size does not change drastically from one material to another. The BJH method was used to calculate the pore size, since this procedure underestimates the size by approximately 1 nm [18]. Very narrow pore size distributions are obtained for all catalysts prepared. In Table 1, even though the materials were synthesized under the same conditions, the amount of TM incorporated varies. The highest loading occurs for Mn and the lowest for Cr. However, the surface area of the Cr-MCM-48 material was found to be the most reduced.

3.2. Analysis of the TM oxidation state, coordination, and location in MCM-48

The location and oxidation state of TM-MCM-48 were investigated by Raman spectroscopy and EPR. The Raman spectra of the TM-MCM-48 are shown in Fig. 4. For Mn-MCM-48, weak bands at 510 and 950 cm^{-1} are observed and can be related to the symmetric and asymmetric stretching modes of Si–O–Mn species in the framework [6,22]. A weak band at 340 cm^{-1} and a strong band at 640 cm^{-1} are also present in Mn-MCM-48 and can be assigned to manganese oxide species within the pores [23]. The EPR spectrum for Mn-MCM-48 (Fig. 5) shows hyperfine splitting originating with Mn^{2+} coupled to its own nuclear spin [7]. The Mn-containing sample shows a signal centered at $g = 2.04$ with an average hyperfine splitting constant of $A = 96$ G. The manganese species present in Mn-MCM-48 as determined by EPR can be assigned to extraframework sites of Mn^{2+} in octahedral symmetry [7].

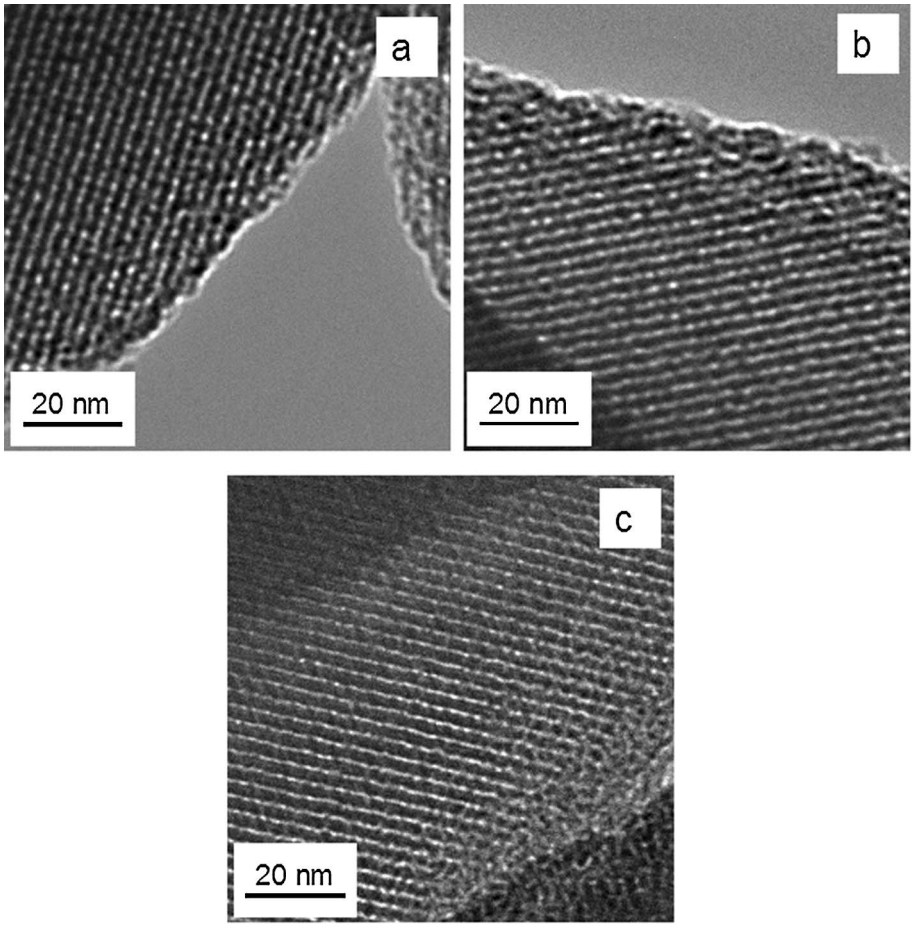

Fig. 2. HRTEM micrographs of TM-MCM-48 materials: (a) Mn-MCM-48, (b) V-MCM-48, and (c) Cr-MCM-48.

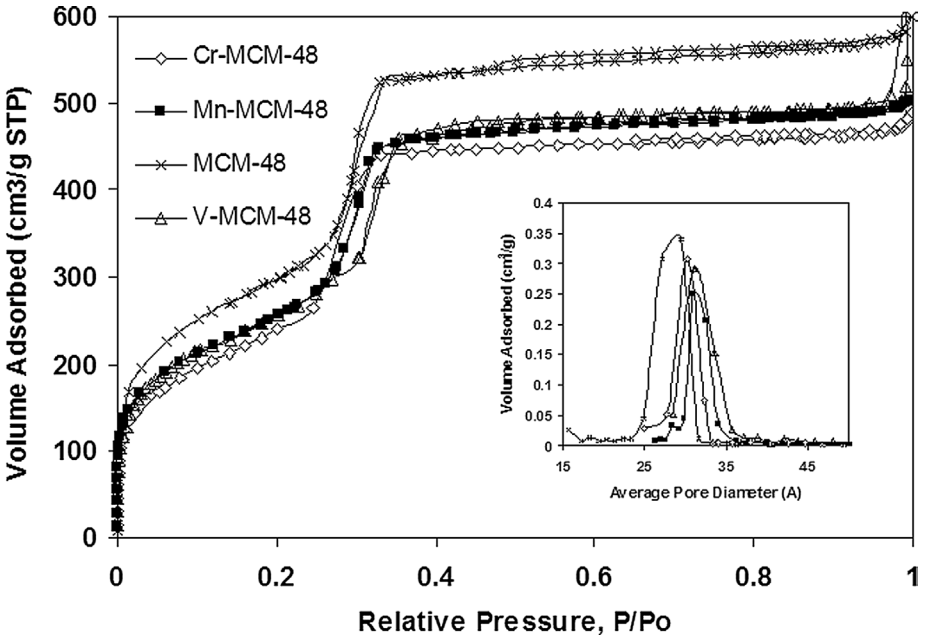

Fig. 3. N_2 adsorption–desorption isotherms and BJH pore size distribution of calcined MCM-48 and TM-MCM-48 materials.

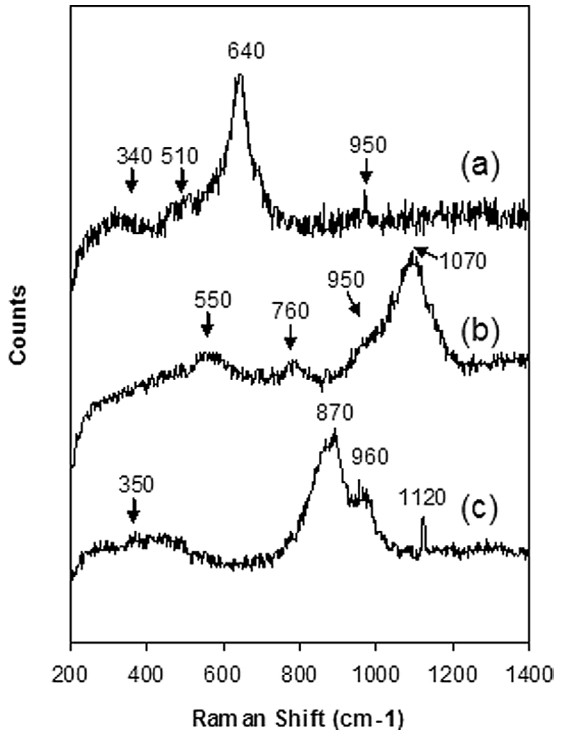

Fig. 4. Raman spectra of (a) Mn-MCM-48, (b) V-MCM-48, and (c) Cr-MCM-48.

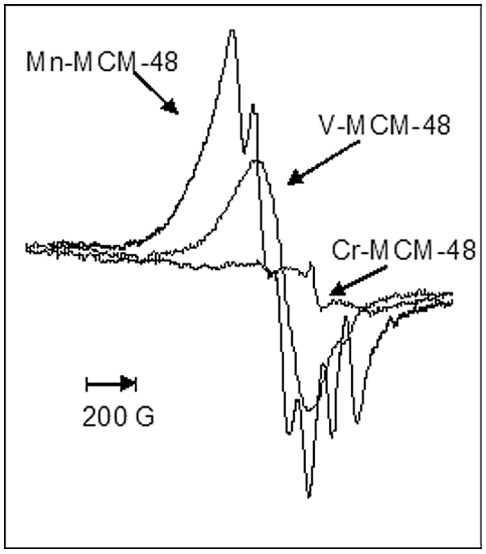

Fig. 5. EPR of TM-MCM-48 materials at room temperature.

Vanadium species in V-MCM-48 studied by Raman show bands at 550, 760, 1070 cm^{-1} and a shoulder around 950 cm^{-1}, as seen in Fig. 4. Broad bands in the 750–1000 cm^{-1} range have been assigned to V–O–V stretches in 2-D polyvanadates [24]. The broad band at 1070 cm^{-1} can be ascribed to the symmetric stretching of terminal V=O bonds of isolated monomeric vanadyl species present in the framework [22]. Raman bands around 930 cm^{-1} are assigned to the V=O symmetric stretching mode of polymerized vanadium oxides in the pores [22]. Thus the shoulder around

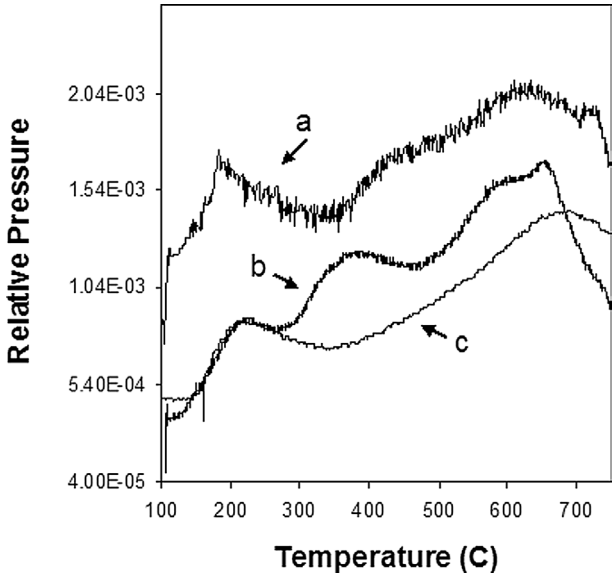

Fig. 6. Acidity profiles by NH_3-TPD of (a) Mn-MCM-48, (b) V-MCM-48, and (c) Cr-MCM-48.

950 cm^{-1} may be due to the presence of extraframework vanadium species. A broad isotropic EPR signal centered at $g = 2.03$ with a peak-to-peak width of 219 G is found for V-MCM-48 (Fig. 6). This EPR signal can be ascribed to the presence of nonisolated V^{4+} clusters of framework vanadium ions [25]; thus the spectrum arises from V^{4+} species coupled by magnetic exchange interactions.

The Raman spectrum of Cr-MCM-48 in Fig. 4 shows a weak band at 350 cm^{-1}, a strong broad band centered around 870 cm^{-1} with a shoulder centered around 960 cm^{-1}, and a sharp band at 1120 cm^{-1}. Bands in the 800–1000 cm^{-1} range observed in chromium oxide dispersed on various supports have been assigned to Cr^{6+} species in the form of chromates with different degrees of oligomerization [26]. Raman bands at 362 and 892 cm^{-1}, and at 960 and 850 cm^{-1}, are related to the presence of hydrated dichromate and trichromate species, respectively [27]. Raman peaks characteristic of Cr_2O_3 species are usually observed around 550 cm^{-1} [28]. The EPR for Cr-MCM-48 shows a very weak signal centered around $g = 1.98$, which can be assigned to Cr^{5+} in square pyramidal coordination [28,29].

3.3. TM-MCM-48 acidity

The acidic properties of TM-MCM-48 materials were investigated by NH_3-TPD; their profiles are shown in Fig. 6. The materials show different acid strength behaviors, depending on the transition metal incorporated. For Mn-MCM-48, desorption peaks are observed around 190, 630, and 730 °C and a shoulder at 630 °C. The Cr-MCM-48 samples show three desorption peaks, at low (230 °C), medium (380 °C), and high (660 °C) temperatures. For Cr-MCM-48 the high temperature peak at 660 °C is accompanied by a broad shoulder located around 600 °C. In V-MCM-48 only two desorption peaks are observed, at 230 and 690 °C. We

Table 2
Results of the catalytic oxidation of styrene with TBHP using different TM-MCM-48 catalysts[a]

Catalyst	Temperature (K)	Styrene conversion (%)	Product selectivity (%)			
			BzA[b]	SO[c]	PhAA[d]	Others
Mn-MCM-48	293	28	74	14	–	12
	318	56	69	21	–	10
	333	56	57	32	3	8
	353	58	59	31	5	5
V-MCM-48	293	21	83	8	–	9
	318	32	85	9	–	10
	333	83	92	5	3	–
	353	84	81	4	9	7
Cr-MCM-48	293	11	62	9	–	29
	318	68	49	26	2	22
	333	68	49	26	2	22
	353	98	47	24	3	26

–, No product was detected.
[a] Reaction time, 24 h.
[b] BzA, benzaldehyde.
[c] SO, styrene oxide.
[d] PhAA, phenylacetaldehyde.

can associate the strength of the acidity with the temperature at which the desorption peak appears. The low-temperature peak is related to weak acid sites, and the high-temperature peak to strong acid sites. Then, Mn- and Cr-containing MCM-48 have at least four sites with weak, medium, and high acid strength. V-MCM-48, on the other hand, shows that only weak and strong acid sites are present.

3.4. Catalytic tests

We have tested the TM-MCM-48 materials in the catalytic oxidation of styrene with TBHP as an oxidant. The catalytic properties of the TM-MCM-48 materials in terms of styrene conversion and product selectivity at different temperatures are presented in Table 2. In all cases benzaldehyde (BzA) and styrene oxide (SO) were the main products. The selectivity for BzA is high for all of the catalysts. In general, the conversion of styrene increased with temperature. An increase in temperature also gives rise to the formation of other products, such as phenylacetaldehyde (PhAA). All of the catalysts are more selective for the formation of benzaldehyde; however, with the V-MCM-48 catalysts the formation of the epoxide product is very low (under 9%), compared with Mn-MCM-48 and Cr-MCM-48. Overall the selectivity of the Cr-MCM-48 is poorer compared with the other catalysts. No significant leaching was detected (<5%) under the reaction conditions studied.

In Table 3 the results of the oxidation reactions with catalysts pretreated at 120 °C for 3 h are reported. We observed considerable improvement in conversion and selectivity with pretreatment of V-MCM-48 catalysts, which reached 100% conversion after only 12 h of reaction. In the case of Mn-MCM-48 and Cr-MCM-48 there seem to be insignificant differences compared with the untreated catalysts.

Table 3
Results of the catalytic oxidation of styrene at 333 K with TBHP using pretreated catalysts[a]

Catalyst	Reaction time (h)	Styrene conversion (%)	Product selectivity (%)		
			BzA[b]	SO[c]	Others
Mn-MCM-48	24	56	69	23	8
Mn-MCM-48	12	51	67	33	–
V-MCM-48	12	100	88	12	–
V-MCM-48	6	59	90	10	–
Cr-MCM-48	12	42	62	16	23

–, No product was detected.
[a] The catalysts were pretreated at 393 K for 4 h.
[b] BzA, benzaldehyde.
[c] SO, styrene oxide.

4. Discussion

4.1. Characterization of TM-MCM-48 materials

The results presented in this work show that all of the TM-MCM-48 materials synthesized maintain the structure and good textural properties (high surface area, narrow pore size distribution) of the host MCM-48. The loading of the TM with the ion-exchange method increases the thermal stability of the silica wall, restricting its contraction. A decrease in the relative intensity of the diffraction peaks was also observed in the presence of the TM with respect to the parent material. The decrease can be attributed to a random distribution of the guest particles in the pores, which lowers the periodicity [10]. The reduction of the intensity can also be due to a dilution of the silica by the presence of the TM as a consequence of a higher adsorption factor for X-rays that TM have in comparison with silicon [30]. The reduction of peak intensity could also be attributed to the partial collapse of the mesoporous structure [31], which is not the case, since XRD and HRTEM show good

preservation of the cubic structure of the mesoporous host. The decreases in surface area and pore volume of the TM-MCM-48 materials with respect to the parent material are consistent with the incorporation of TM within the pores. Reversible adsorption-desorption isotherms are observed for all of the TM-MCM-48 materials prepared. Reversibility of the isotherm implies that there is negligible obstruction of the pore channels [32]. The fact that the incorporation of the TM takes place in the presence of surfactant species in the pores restricts the location of the TM and avoids clogging of the channels [10,17].

The results obtained for the analysis of the manganese species in Mn-MCM-48 showed that Mn is present in the mesoporous material as a mixed-valence system, and mainly located in the pores rather that in the silica framework [17]. In a previous report XPS was also used to analyze the binding energy (BE) values corresponding to MnMCM-48; the values obtained for Mn-MCM-48 agree with those for mixed-valence manganese oxide systems. The calculated average oxidation state (AOS) of the Mn species present in Mn-MCM-48 prepared under conditions similar to those in this work was determined to be 3.4, which is consistent with a manganese mixed-valence system [17].

Chromium species in Cr-MCM-48 appear to be present as Cr^{6+} hydrated dichromate and trichromate species with different degrees of oligomerization. EPR, on the other hand, gives a signal that could be associated with the presence of Cr^{5+} as $(Cr{=}O)^{3+}$ in the mesoporous structure [29]. Some authors have concluded that low loadings of Cr in supports generate mostly monomeric isolated species, and at high loadings the formation of polymerized species is favored [26]. Cr^{6+}, Cr^{5+}, and Cr_2O_3 clusters are likely to form on calcined surfaces, and their coordination geometries strongly depend on the support type and composition. Because chromium has a complex redox and coordination chemistry, along with the presence of the silica support, it is difficult to understand the nature of the chromium species present. However, during calcinations in which silica supports are used, chromium species can anchor to the silica support and react with the hydroxyl groups of the inorganic oxide to form surface Cr^{6+} species [29,33]. Nevertheless, under calcination conditions with silica surfaces, Cr_2O_3 can also be formed [29,33]. Even though it is difficult to determine the nature of the chromium species in Cr-MCM-48, Raman and EPR data indicate that a mixture of different valences and coordination environments are present.

The vanadium species seem to be present as a mixed system as well. The intensities of the Raman bands at 950 and 1070 cm^{-1} have been associated with the amount of isolated or polymeric vanadium species, respectively. In our case the intensity of the band at 950 cm^{-1} is stronger, which could indicate that a larger amount of isolated species is present in the MCM-48 host. In M41S materials Raman bands around 500 cm^{-1} have been ascribed to the motion of the bridge oxygen connecting the two atoms of a T–O–T bridge [34] and associated with vanadium in the framework. The EPR, on the other hand, shows a signal associated with V^{4+} in framework sites. Thus, vanadium in V-MCM-48 is present as different isolated, polymeric, and framework species.

4.2. Catalytic performance

All of the TM-MCM-48 materials are active in the catalytic epoxidation of styrene. However, the selectivity of all of the catalysts for BzA from styrene is higher than for SO, particularly for the vanadium catalyst. The conversion for all of the materials increases with temperature, as expected. For Mn-MCM-48 the amount of styrene converted doubles from room temperature to 318 K and at higher temperatures appears to reach a maximum. Of all three catalysts, Mn-MCM-48 showed the highest selectivity ($\sim$ 30%) for styrene oxide. In the case of V-MCM-48, the catalyst seems to reach a maximum conversion at 333 K, with poor selectivity for SO. However, when the vanadium catalysts were pretreated, a considerable improvement in conversion of substrate (100%) was found, after only 12 h of reaction. This can indicate that the active sites of the V-MCM-48 catalyst are affected by water adsorbed to the surface. The selectivity of product remains practically the same with a slight improvement to SO, and no formation of other products.

In the case of Mn-MCM-48 and Cr-MCM-48, no significant improvement with pretreatment is found. Other authors have also found higher selectivity for BzA in vanadium-containing MCM-41 materials [35]. The formation of BzA from styrene can occur by two different routes. One possible pathway is the oxidation of the side chain, which causes breaking of the C=C bond to form BzA. Another way to form BzA from styrene is by an epoxidation reaction to form SO, which further forms BzA in the presence of peroxide. The two different pathways may be occurring in parallel; however, for the vanadium catalyst the oxidative cleavage of styrene may be favored. The difference in catalytic behavior between the manganese and vanadium catalyst in terms of selectivity for BzA and SO is probably due to the nature of the active centers. The Mn-MCM-48 acidity profile (Fig. 6) is quite different from the vanadium catalyst and favors the epoxidation reaction. Small amounts ($>$ 9%) of PhAA are produced when the reaction temperature is increased. The chromium catalyst, on the other hand, shows the poorest catalytic behavior in terms of selectivity, especially at higher temperatures ($>$ 60 °C), where products other than BzA, SO, and PhAA are formed. Mn-MCM-48 and Cr-MCM-48 catalysts require lower temperature (318 K) to achieve their maximum conversion. The TM-MCM-48 systems studied have different acidity profiles, which can be associated with their different catalytic behavior. The activities of framework and extraframework transition metals present in supported materials toward the formation of particular species in different catalytic reactions have been studied [29,36,37]. Framework Nb ions located in the framework have been found to be more selective for the formation of BzA. Although Nb extraframework ions are also active in

the oxidation of styrene, they appear to be less active than Nb in the framework [37]. Iron species present in the framework of MCM-41 materials were shown to be more active for the epoxidation of styrene, as opposed to Fe present in extraframework positions [36]. In our case, the epoxidation reaction appears to be favored when the Mn-MCM-48 and Cr-MCM-48 catalyst are used. For the Mn catalyst the manganese species are mainly located in extraframework sites. Further studies on the nature of the reaction pathways in the oxidation of styrene with the TM-MCM-48 materials need to be performed.

5. Conclusions

TM-MCM-48 materials containing Mn, V, and Cr were successfully synthesized by the anion-exchange method. Characterization of the TM-MCM-48 materials showed good preservation of the structural and textural properties of the mesoporous host. All of the catalysts showed very good conversion and selectivity in the oxidation of styrene. The activity of the catalysts in the oxidation of styrene seems to be associated with the composition of these catalysts. V-MCM-48 showed the highest conversion, reaching 100% consumption of the substrate with high selectivity (88%) for BzA. On the other hand, Mn-MCM-48 and Cr-MCM-48 catalysts showed a much better selectivity for the formation of the epoxide, 30 and 26%, respectively, compared with only 12% selectivity for SO by V-MCM-48. However, lower conversions are achieved with the Mn and Cr catalysts. Since no significant leaching was observed, the catalysts may be reused.

Acknowledgments

We thank the US Department of Energy, Geosciences and Biosciences Division, Office of Basic Energy Sciences, Office of Science, for financial support. We also thank the Institute of Materials Science and Dr. M. Aindow for providing access to electron microscopy facilities and Mr. Jason Durand for helpful discussions.

References

[1] C.T. Kresge, M.E. Leonowicz, W.J. Roth, J.C. Vartulli, J.S. Beck, Nature 359 (1992) 710.
[2] J.Y. Ying, C.P. Mehnert, M.S. Wong, Angew. Chem., Int. Ed. 38 (1999) 56.
[3] A. Corma, M.T. Navarro, J. Pérez-Pariente, J. Chem. Soc., Chem. Commun. (1994) 147.
[4] B.J. Aronson, C.F. Blanford, A. Stein, Chem. Mater. 9 (1997) 2842.
[5] Z.Y. Yuan, W. Zhou, Z.L. Zhang, J.Q. Liu, J.Z. Wang, H.X. Li, L.M. Peng, Surf. Interface Catal. 32 (2001) 193.
[6] Q. Zhang, Y. Wang, S. Itsuki, T. Shishido, K. Takehira, J. Mol. Catal. A 188 (2002) 189.
[7] D.Y. Zhao, D.J. Goldfarb, J. Chem. Soc., Chem. Commun. (1995) 875.
[8] M. Yonemitsu, Y. Tanaka, M. Iwamoto, Chem. Mater. 9 (1997) 2679.
[9] J. Xu, Z. Luan, M. Hartman, L. Kevan, Chem. Mater. 11 (1999) 2928.
[10] B.J. Aronson, C.F. Blanford, A. Stein, J. Phys. Chem. B 104 (2000) 449.
[11] V. Caps, S.C. Tsang, Catal. Today 61 (2000) 19.
[12] W. Zhang, T.J. Pinnavaia, Catal. Lett. 38 (1996) 261.
[13] E.P. Reddy, J. Phys. Chem. B 106 (2002) 3394.
[14] C. Pak, G.L. Haller, Micropor. Mesopor. Mater. 48 (2001) 165.
[15] E.P. Reddy, L. Davydov, P.G. Smirniotis, J. Phys. Chem. B 106 (2002) 3394.
[16] N. Lang, P. Delichere, A. Tuel, Micropor. Mesopor. Mater. 56 (2002) 203.
[17] S. Gómez, O. Giraldo, L.J. Garcés, J. Villegas, S.L. Suib, Chem. Mater. 16 (2004) 2411.
[18] K. Schumacher, P.I. Ravikovitch, A. Du Chesne, A.V. Neimark, K.K. Unger, Langmuir 16 (2000) 4648.
[19] M. Fröba, R. Köhn, B. Gaellë, Chem. Mater. 11 (1999) 2858.
[20] J.C. Vartulli, K.D. Schmitt, C.T. Kresge, W.J. Roth, M.E. Leonowicz, S.B. McCullen, S.D. Hellring, J.S. Beck, J.L. Schlenker, D.H. Olsen, E.W. Sheppard, Chem. Mater. 6 (1994) 2317.
[21] K.S.W. Sing, D.H. Everet, R.A.W. Haul, L. Moscov, R.A. Pierotti, J. Rouquérol, T. Siemieniewska, Pure Appl. Chem. 57 (1985) 603.
[22] C. Li, J. Catal. 216 (2003) 203.
[23] R. Radhakrishnan, T.S. Oyama, J.G. Chen, K. Asakura, J. Phys. Chem. B 105 (2001) 4245.
[24] N. Magg, B. Immaraporn, J.B. Giorgi, T. Schroeder, M. Bäumer, J. Döbler, Z. Wu, E. Kondratenko, M. Cherian, M. Baerns, P.C. Stair, J. Sauer, H. Freund, J. Catal. 226 (2004) 88.
[25] M. Mathieu, P. Van Der Voort, B.M. Weckhuysen, R.R. Rao, G. Catana, R.A. Schoonheydt, E.F. Vansant, J. Phys. Chem. B 105 (2001) 3393.
[26] B. Grzybowska, J. Słoczyński, R. Grabowski, K. Wcisło, A. Kozłowska, J. Stoch, J. Zieliński, J. Catal. 178 (1998) 687.
[27] M.A. Vuurman, I.E. Wachs, J. Phys. Chem. 96 (1992) 5008.
[28] Z. Zhu, M. Hartmann, E.M. Maes, R.S. Czernuszewicz, L. Kevan, J. Phys. Chem. B 104 (2000) 4690.
[29] B.M. Weckhuysen, I.E. Wachs, R.A. Schoonheydt, Chem. Rev. 96 (1996) 3327.
[30] L. Vradman, M.V. Landau, M. Herskowitz, V. Ezersky, M. Talianker, S. Nikitenko, Y. Koltypin, A. Gedanken, J. Catal. 213 (2003) 163.
[31] J. Evans, A.B. Zaki, M.Y. El-Sheikh, S.A. El-Safty, J. Phys. Chem. B 104 (2000) 10271.
[32] H. Yang, G. Vovk, N. Coombs, I. Sokolov, G.A. Ozin, J. Mater. Chem. 8 (1998) 743.
[33] P.C. Thüne, R. Linke, W.J.H. van Gennip, A.M. de Jong, J.W. Niemantsverdriet, J. Phys. Chem. B 105 (2001) 3073.
[34] E. Geidel, H. Lechert, J. Döbler, H. Jobic, G. Calzaferri, F. Bauer, Micropor. Mesopor. Mater. 65 (2003) 31.
[35] V. Parvulescu, C. Anastasescu, C. Constantin, B.L. Su, Catal. Today 78 (2003) 477.
[36] Y. Wang, Q. Zhang, T. Shishido, K. Takehira, J. Catal. 209 (2002) 186.
[37] V. Parvulescu, C. Constantin, B.L. Su, J. Mol. Catal. A: Chem. 202 (2003) 171.